

# Deposition of highly oriented lanthanum nickel oxide thin film on silicon wafer by CSD

H. Suzuki<sup>a,\*</sup>, T. Naoe<sup>a</sup>, H. Miyazaki<sup>b</sup>, T. Ota<sup>c</sup>

<sup>a</sup> Graduate School of Science and Technology, Shizuoka University, 3-5-1 Johoku, Hamamatsu, Shizuoka 432-8561, Japan

<sup>b</sup> Interdisciplinary Faculty of Science and Engineering, Shimane University, 1060 Nishikawatsu, Matsue, Shimane 690-8504, Japan

<sup>c</sup> Ceramics Research Laboratory, Nagoya Institute of Technology, 10-6-29 Asahigaoka, Tajimi, Gifu 507-0071, Japan

Available online 21 March 2007

## Abstract

This paper describes the orientation control and the electrical properties of the chemical solution deposition (CSD) derived  $\text{LaNiO}_3$  (LNO) thin film. The LNO precursor solutions were prepared using lanthanum nitrate and nickel acetate as La and Ni source, and ethanol or 2-methoxyethanol and 2-aminoethanol mixed solution as solvents. The LNO films were spin-coated using these precursor solutions and annealed at the temperature from 500 to 700 °C. The resulting LNO film annealed at 700 °C derived from 2-methoxyethanol and 2-aminoethanol mixed solvent exhibited (1 0 0)-orientation, with some surface cracks and pores, and relatively higher resistivity of  $2.49 \times 10^{-3} \Omega \text{ cm}$ . The LNO film derived from 2-methoxyethanol and 2-aminoethanol mixed solvent annealed at 700 °C in an oxygen atmosphere showed highly (1 0 0)-orientation, with higher density, a few cracks and pores, and exhibited a good electrical resistivity of  $7.27 \times 10^{-4} \Omega \text{ cm}$ .

© 2007 Elsevier Ltd. All rights reserved.

**Keywords:** Chemical solution deposition; Films

## 1. Introduction

Lead zirconate titanate (PZT) films have been widely studied with great interest for their applications in memory devices, pyroelectric sensors and microactuators.<sup>1,2</sup> Platinum (Pt) film is usually used as an electrode for ferroelectric capacitors. However, using Pt film as a ferroelectric device electrode, we observed serious fatigue over the region of  $10^6$  switching cycles.<sup>3,4</sup> To improve this fatigue property, various perovskite oxides with low resistivity, which include  $\text{YBa}_2\text{Cu}_3\text{O}_{7-x}$ ,<sup>5</sup>  $(\text{La,Sr})\text{CoO}_3$ ,<sup>6</sup>  $\text{LaNiO}_3$  (LNO),<sup>7</sup> and  $\text{SrRuO}_3$ ,<sup>8</sup> have been studied as Pt electrode replacements.

The actual LNO crystal structure is rhombohedral. However, it can be considered as a pseudo cubic perovskite structure<sup>9,10</sup> with the lattice constant of 0.384 nm. In this study, we postulated the LNO crystal structure as pseudo cubic (JCPDS 33-0710). Because the lattice constants of the  $\text{Pb}_{0.52}\text{Zr}_{0.48}\text{TiO}_3$  are  $a=0.404$  nm and  $b=0.415$  nm (JCPDS 43-0472), respectively, nearly equivalent to that of the LNO, PZT thin films on the LNO thin film electrode are expected to grow epitaxi-

ally, leading to the excellent electrical properties. In addition, a resistivity of LNO is expected to show in the range from 5 to  $10 \times 10^{-4} \Omega \text{ cm}$ .<sup>11-13</sup> For these reasons, LNO is a promising candidate for a thin film electrode of PZT thin films.

In the previous studies, we prepared conductive LNO films by a chemical solution deposition (CSD)<sup>14,15</sup> using mixed solvent of 2-amino ethanol and 2-methoxy ethanol. The film orientation of the resultant LNO was successfully controlled to (1 0 0)- or (1 1 0)-direction by changing the concentration of the precursor solution or solvent for a precursor solution.<sup>14,15</sup> Aims of this work are the deposition of LNO films with preferred orientation, high dense, flat surface and low resistivity by choosing the precursor solution solvent, annealing conditions and annealing atmospheres. In addition, we discussed an orientation mechanism accompanied with the kind of solvents and annealing conditions.

## 2. Experimental procedure

Lanthanum nitrate and nickel acetate were used as raw materials for the LNO precursor solution, and ethanol or 2-methoxyethanol and 2-aminoethanol mixed solution was used as a solvent. Details of the precursor solution preparation are described in the previous papers.<sup>14,15</sup>

\* Corresponding author. Tel.: +81 53 478 1157; fax: +81 53 478 1157.  
E-mail address: [tchsuzu@ipc.shizuoka.ac.jp](mailto:tchsuzu@ipc.shizuoka.ac.jp) (H. Suzuki).

An LNO precursor film was deposited on the Si substrate by spin coating using 0.3 M LNO solutions. The precursor LNO film was dried at 150 °C for 10 min, pre-annealed at 350 °C for 10 min, followed by the heating at 500 °C for 10 min to remove residual organics. Finally, the film was annealed at temperatures from 500 to 700 °C for 5 min using Rapid Thermal Annealing (RTA). These processes were repeated to increase the film thickness of the resultant LNO up to 300 nm in thickness.

Thermogravimetric and differential thermal analysis were performed on the dried LNO precursor powders using Rigaku thermoplus2 TG8120. The crystal structure of the obtained LNO films was characterized by X-ray diffraction using Rigaku RINT 2200 with Cu K $\alpha$  radiation. The surface morphology of the LNO films was investigated by a scanning electron microscope (SEM) using Jeol JSM-5600 and by an atomic force microscopy (AFM) using Seiko Instruments SPI3800N. Resistivity of the films was measured by a four-point probe method using Hewlett-Packard HP-34401A.

### 3. Results and discussion

#### 3.1. Decomposition and crystallization of LNO precursors

LNO precursor solution could be prepared from lanthanum nitrate and nickel acetate as La and Ni sources, and ethanol or 2-methoxyethanol and 2-aminoethanol mixed solution as solvents (hereinafter, we designate the 2-methoxyethanol and 2-aminoethanol mixed solution as “mixed solvent”). LNO precursor powders were prepared by drying the solutions gradually at 150 °C in air for 24 h. Fig. 1 shows the results of the TG-DTA

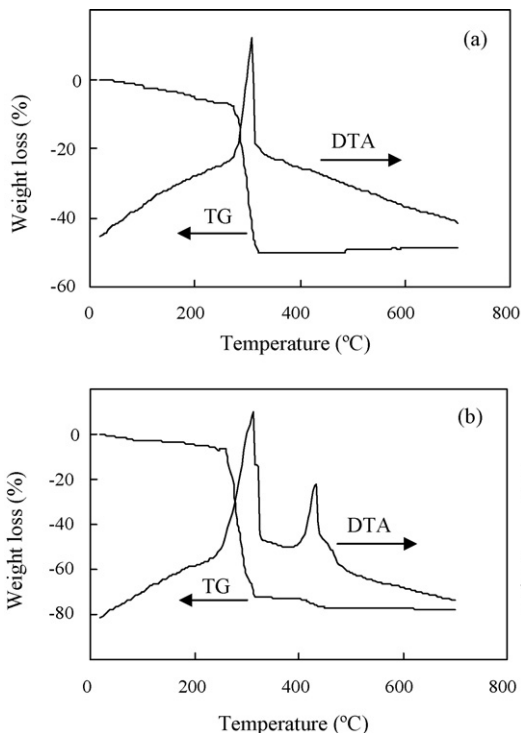


Fig. 1. TG-DTA curves for the LNO powder derived from (a) ethanol and (b) 2-methoxyethanol and 2-aminoethanol mixed solution solvents.

for the dried LNO precursor powders, which were derived from the LNO solution using (a) an ethanol solvent and (b) a mixed solvent. As shown in Fig. 1(a), one step of weight loss was observed at 300 °C for the LNO precursor powder using ethanol solvent. It assumed that the amount of the weight loss in TG curves was ascribed to the burn out of the residual organics. On the other hand, two steps of weight loss associated with the two exothermic peaks were observed at around 300 and 450 °C for the LNO precursor powder using mixed solvent (Fig. 1(b)). In addition, the weight loss of the LNO precursor powder derived from mixed solvent exhibited higher value of about 80% (see Fig. 1(b)), which value was much larger than that derived from ethanol solvent of 50% (see Fig. 1(a)). It proved that the LNO precursor powder derived from mixed solvent included a large amount of organics compared with that of the powder derived from ethanol solvent.

In order to clarify the two steps of weight loss in the LNO precursor powder as well as to investigate the crystallization process, crystalline phases were identified by XRD for the powders annealed at various temperatures derived from the different solvents (Fig. 2). From Fig. 2(a), La<sub>2</sub>O<sub>3</sub> and NiO phases were

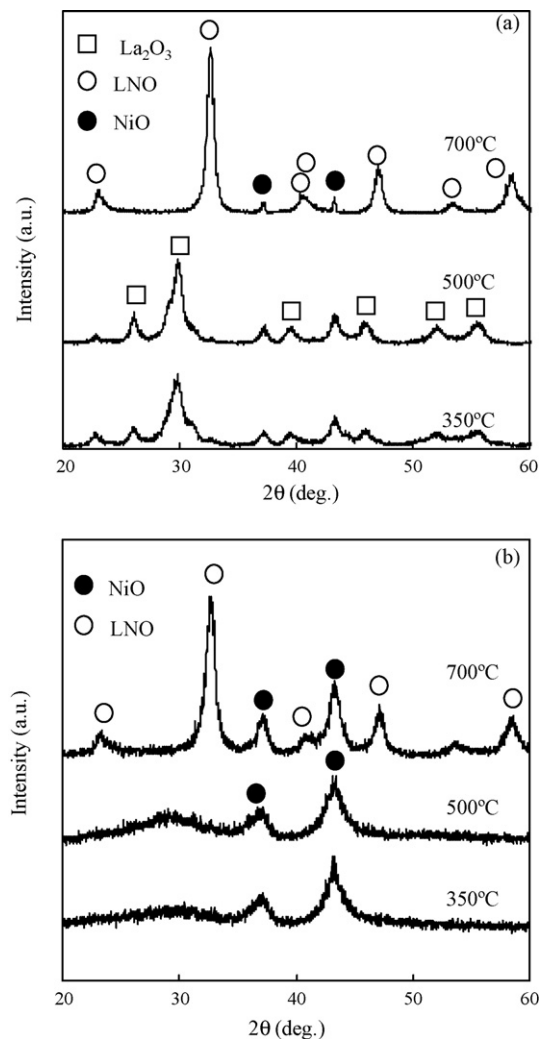


Fig. 2. XRD patterns for the annealed LNO powder derived from (a) ethanol and (b) 2-methoxyethanol and 2-aminoethanol mixed solution solvents.

identified in the powder derived from ethanol solvent below 500 °C. In contrast, only a NiO phase was observed in the powder from mixed solvent if annealed below 500 °C. Namely, the LNO phase crystallized by the reaction between  $\text{La}_2\text{O}_3$  and NiO phases for the precursor powder from ethanol solvent, whereas the LNO phase crystallized by the reaction between more homogeneous  $\text{La}_2\text{O}_3$  rich amorphous phase and NiO for the case of the precursor powder from mixed solvent (Fig. 2(b)). From these results, the former peak of the two steps weight loss for the LNO precursor powder from mixed solvent was ascribed to the loss of the burn out of the residual organics, and the latter one could be ascribed to the crystallization of the LNO phase at higher temperature.

### 3.2. Deposition of LNO film

The LNO precursor films were spin-coated using the precursor solutions with ethanol and mixed solvents, and these films were annealed at temperatures from 500 to 700 °C in air. Fig. 3 showed the XRD patterns for the obtained LNO films derived from (a) ethanol and (b) 2-methoxyethanol and 2-aminoethanol mixed solvent. The perovskite LNO films with random orientation were obtained for the case of the precursor derived from ethanol at above the annealing temperature of 600 °C, and the perovskite LNO films with strong (100)-orientation were

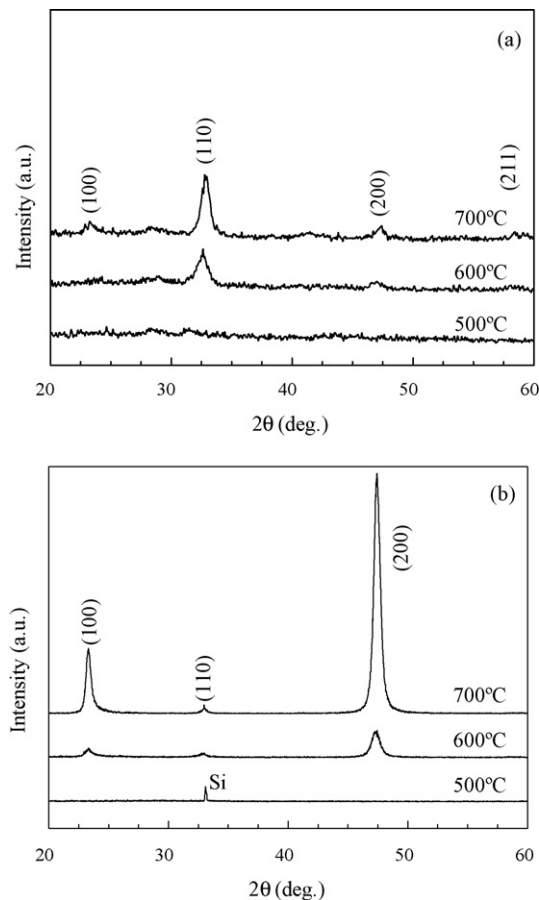


Fig. 3. XRD patterns for the LNO films derived from (a) ethanol and (b) 2-methoxyethanol and 2-aminoethanol mixed solution solvents.

deposited at above the temperature of 600 °C if the mixed solvent was used for a precursor solution. On the other hand, the LNO films exhibited relatively good crystallinity if annealed at 700 °C, independent of the solvent used.

In order to observe the surface morphology and to clarify the orientation mechanism, AFM observation was carried out for the resultant LNO films annealed at 700 °C (Fig. 4). As shown in Fig. 4(a), the LNO film prepared using ethanol solvent was very dense, and the LNO primary particles were very fine. From Figs. 1(a) and 2(a), it assumed that  $\text{La}_2\text{O}_3$  and NiO crystals were formed in the LNO precursor film at the annealing temperatures below 500 °C if ethanol solvent was used. The formed  $\text{La}_2\text{O}_3$  crystals reacted with NiO in the precursor films at temperature above 500 °C to form the crystalline LNO with small particle size and random orientation. On the other hand, the LNO film deposited from mixed solvent exhibited some cracks and

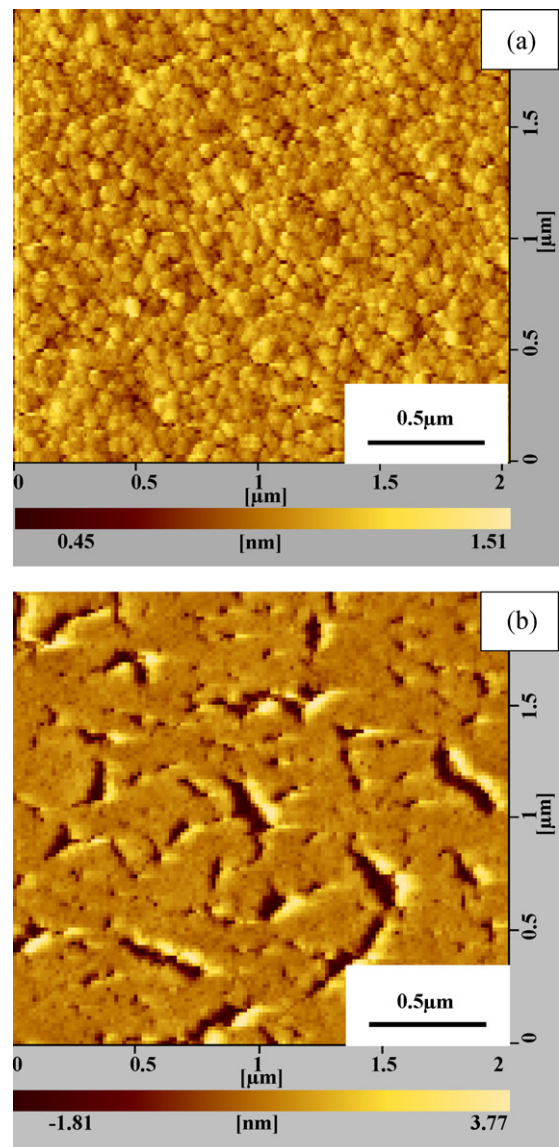


Fig. 4. AFM images of the resultant LNO films derived from different solvent of (a) ethanol and (b) 2-methoxyethanol and 2-aminoethanol mixed solution solvents.

pores (Fig. 4(b)). The LNO precursor film deposited from mixed solvent included considerable organics at relatively high temperatures below 400 °C (from Fig. 1(b)). A large amount of residual organics could be burnt out at relatively high annealing temperatures above 400 °C in the LNO precursor film, leading to a lot of cracks or pores in the resultant LNO film from the mixed solvent. In addition, from Figs. 1(b) and 2(b), it assumed that a faint amount of NiO phase was found in the LNO precursor film from mixed solvent at the relatively low annealing temperature below 500 °C, suggesting the relatively homogeneous reaction between fine NiO nucleus and the more homogeneous La<sub>2</sub>O<sub>3</sub> rich amorphous phase in the LNO film at relatively higher annealing temperatures above 500 °C. The (100)-plane of LNO has the smallest surface energy, and could grow parallel to the substrate surface.<sup>16</sup> In addition, thermodynamically stable (100)-plane could be grown if the crystallization occurred at higher temperature to show a preferred orientation of the deposited LNO film derived from mixed solvent.

The LNO precursor films were annealed in oxygen atmosphere at 700 °C to remove a residual organics effectively in the films, especially for the case of films derived from mixed solvent. Fig. 5 shows the SEM images of the LNO films annealed at 700 °C in air and in oxygen, respectively. There are few cracks and pores on the LNO film surface annealed in the oxygen atmosphere in contrast to those of the LNO film surface annealed in air. Resistivity of the LNO film annealed in air and oxygen atmosphere was  $2.49 \times 10^{-3}$  and

$7.27 \times 10^{-4} \Omega \text{ cm}$  at room temperature, respectively. Therefore, it was concluded that annealing in oxygen atmosphere is very effective to remove the residual organics in the LNO precursor film, which crystallizes at higher temperature, leading to the preferred orientation. The resistivity of the LNO film annealed at 700 °C in oxygen was close to the value on the previous reports.<sup>11–13</sup> Huang and Yao<sup>11</sup> reported that the resistivity of the LNO film deposited by mist plasma evaporation decreased in the range from  $2.54 \times 10^{-3}$  to  $7.7 \times 10^{-4} \Omega \text{ cm}$  after being annealed at in air, and they described that LNO film deposited under the sufficient oxygen atmosphere could show enough low values of resistivity. Sanchez et al.<sup>17</sup> reported that the resistivity of the LNO film prepared by pulsed laser deposition decreased with the increase of oxygen pressure, and this tendency depended on the oxygen deficiency of the resultant LNO film. We assumed that annealing in oxygen atmosphere not only yielded dense and flat surface but also improved an electrical resistivity to reduce the oxygen deficiency in the resultant LNO film in this study.

#### 4. Conclusion

The LNO precursor solutions were prepared by lanthanum nitrate and nickel acetate as La and Ni source, and ethanol or 2-methoxyethanol and 2-aminoethanol mixed solution as solvent. The (100)-oriented LNO film could be deposited from the LNO precursor solution of 2-methoxyethanol and 2-aminoethanol mixed solvent. The LNO film annealed in oxygen atmosphere exhibited relatively dense microstructure as well as the enough low resistivity of  $7.27 \times 10^{-4} \Omega \text{ cm}$  for the oxide thin film electrode.

#### Acknowledgement

This work was supported in part by Grants-in-Aid for Scientific Research (B) (No. 16360325) from Japan Society for the promotion of Science.

#### References

1. Talor, D. V. and Damjanovic, D., Piezoelectric properties of rhombohedral Pb(Zr,Ti)O<sub>3</sub> thin films with (100), (111), and “random” crystallographic orientation. *Appl. Phys. Lett.*, 2000, **76**, 1615–1617.
2. Du, X., Zheng, J., Belegundu, U. and Uchino, K., Crystal orientation dependence of piezoelectric properties of lead zirconate titanate near the morphotropic phase boundary. *Appl. Phys. Lett.*, 1998, **72**, 2421–2423.
3. Amanuma, K., Hase, T. and Miyasaka, Y., Fatigue characteristics of sol-gel derived Pb(Zr,Ti)O<sub>3</sub> thin films. *Jpn. J. Appl. Phys.*, 1994, **33**, 5211–5214.
4. Al-Shareef, H. N., Bellur, K. R., Auciello, O., Chen, X. and Kingon, A. I., Effect of composition and annealing conditions on the electrical properties of Pb(Zr<sub>x</sub>Ti<sub>1-x</sub>)O<sub>3</sub> thin films deposited by the sol-gel process. *Thin Solid Films*, 1994, **252**, 38–43.
5. Kurogi, H., Yamagata, Y., Ebihara, K. and Inoue, N., Preparation of PZT thin films on YBCO electrodes by KrF excimer laser ablation technique. *Surf. Coat. Technol.*, 1998, **100–101**, 424–427.
6. Ramesh, R., Gilchrist, H., Sands, T., Keramidis, V. G., Haakennasen, R. and Fork, D. K., Ferroelectric La-Sr-Co-O/Pb-Zr-Ti-O/La-Sr-Co-O heterostructures on silicon via template growth. *Appl. Phys. Lett.*, 1993, **63**, 3592–3594.

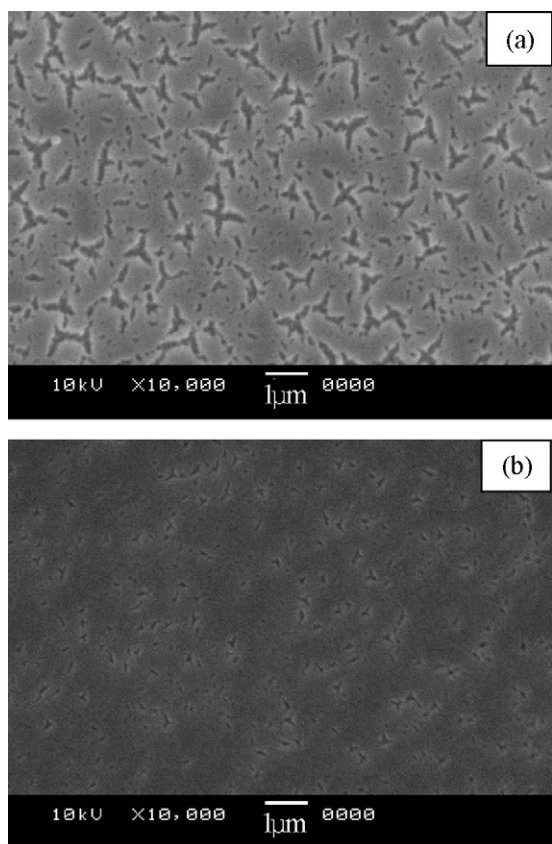


Fig. 5. SEM images of the resultant LNO films derived from mixed solvent, annealed in (a) air and (b) oxygen atmosphere.

7. Jiankang, L. and Xi, Y., Microstructure and electrical properties of  $\text{Pb}(\text{Zr}_{0.52}\text{Ti}_{0.48})\text{O}_3$  ferroelectric films on different bottom electrodes. *Mater. Lett.*, 2004, **58**, 3447–3450.
8. Morimoto, T., Hidaka, O., Yamakawa, K., Arisumi, O., Kanaya, H., Iwamoto, T. et al., Ferroelectric properties of  $\text{Pb}(\text{Zi,Ti})\text{O}_3$  capacitor with thin  $\text{SrRuO}_3$  films within both electrodes. *Jpn. J. Appl. Phys.*, 2000, **39**, 2110–2113.
9. Zhong, X. L., Lu, L. and Lai, M. O., Growth of highly orientated  $0.65\text{Pb}(\text{Mg}_{1/3}\text{Nb}_{2/3})\text{O}_3-0.35\text{PbTiO}_3$  films by pulsed laser deposition. *Surf. Coat. Technol.*, 2005, **198**, 400–405.
10. Zhu, T. J., Lu, L. and Thompson, C. V., Growth and properties of (001)-oriented  $\text{Pb}(\text{Zr}_{0.52}\text{Ti}_{0.48})\text{O}_3/\text{LaNiO}_3$  films on Si(001) substrates with TiN buffer layers. *J. Cryst. Growth*, 2004, **273**, 172–178.
11. Huang, H. and Yao, X., Preparation of  $\text{LaNiO}_3$  thin films by mist plasma evaporation. *Thin Solid Films*, 2004, **462–463**, 123–126.
12. Wakiya, N., Azuma, T., Shinozaki, K. and Mizutani, N., Low-temperature epitaxial growth of conductive  $\text{LaNiO}_3$  thin films by RF magnetron sputtering. *Thin Solid Films*, 2002, **410**, 114–120.
13. Meng, X.-J., Sun, J.-L., Yu, J., Ye, H.-J., Guo, S.-L. and Chu, J.-H., Preparation of highly (100)-oriented metallic  $\text{LaNiO}_3$  films on Si substrates by a modified metalorganic decomposition technique. *Appl. Surf. Sci.*, 2001, **171**, 68–70.
14. Miyazaki, H., Goto, T., Miwa, Y., Ohno, T., Suzuki, H., Ota, T. et al., Preparation and Evaluation of  $\text{LaNiO}_3$  thin film electrode with chemical solution deposition. *J. Eur. Ceram. Soc.*, 2004, **24**, 1005–1008.
15. Suzuki, H., Miwa, Y., Naoe, T., Miyazaki, H., Ota, T., Fuji, M. et al., Orientation control and electrical properties of PZT/LNO capacitor through chemical solution deposition. *J. Eur. Ceram. Soc.*, 2006, **26**, 1953–1956.
16. Miyake, S., Fujihara, S. and Kimura, T., Characteristics of oriented  $\text{LaNiO}_3$  thin films fabricated by the sol–gel method. *J. Eur. Ceram. Soc.*, 2001, **21**, 1525–1528.
17. Sanchez, F., Ferrater, C., Alcobe, X., Bassas, J., Garcia-Cuenca, M. V. and Varela, M., Pulsed laser deposition of epitaxial  $\text{LaNiO}_3$  thin films on buffered Si(100). *Thin Solid Films*, 2001, **384**, 200–205.